

## Article

# Study on Temperature Distribution along the Ultra-Long Underwater Tunnel: Based on the Long-Term Measured Results of the Shanghai Yangtze River Tunnel

Jun Gao <sup>1</sup>, Weichen Guo <sup>1</sup>, Mingyao Ma <sup>1</sup>, Yumei Hou <sup>1</sup>, Ruiyan Zhang <sup>2</sup>, Lingjie Zeng <sup>1,\*</sup>, Chengquan Zhang <sup>1</sup>, Yukun Xu <sup>1</sup>, Xiaobin Wei <sup>1</sup> and Changsheng Cao <sup>1</sup>

<sup>1</sup> School of Mechanical Engineering, Tongji University, Shanghai 200092, China; gaojun-hvac@tongji.edu.cn (J.G.); weichen\_guo@foxmail.com (W.G.); 2130269@tongji.edu.cn (M.M.); houyumei1991@163.com (Y.H.); 1410306@tongji.edu.cn (C.Z.); 2110430@tongji.edu.cn (Y.X.); 2010349@tongji.edu.cn (X.W.); cao\_changsheng@163.com (C.C.)

<sup>2</sup> School of Environment and Architecture, University of Shanghai for Science and Technology, Shanghai 200093, China

\* Correspondence: zenglingjie@tongji.edu.cn

**Abstract:** Tunnels play a vital role in enhancing traffic flow and supporting public transportation systems. However, the discharge of polluted air and waste heat from vehicles passing through tunnels significantly raises the temperature inside, presenting challenges in terms of occupant comfort, tunnel safety, and infrastructure integrity. Therefore, ensuring proper temperature control is essential for their efficient operation. This study aims to investigate the phenomenon of temperature rise in ultra-long tunnels during normal operations, as limited research has been conducted in this area. The Shanghai Yangtze River Tunnel serves as a case study, utilizing temperature and air velocity data collected throughout the year (2021) from the management company. The analysis reveals that the temperature distribution near the tunnel exit is influenced by outdoor temperature fluctuations and traffic volume. The highest temperatures occur on 25 August (39.74 °C) during peak traffic hours. On-site measurements of tunnel temperature, humidity, and air velocity during winter and summer seasons yield the following results. During winter, the air temperature and wall temperature inside the tunnel experience significant increases along its length. The air temperature rises by approximately 11 °C from the entrance to the exit, while the wall temperature increases by about 15 °C. In contrast, during summer, the air temperature only rises by 2.7 °C, and the wall temperature increases by around 3 °C. Consequently, the humidity decreases along the tunnel, and this decrease is correlated with the magnitude of temperature increase. Furthermore, measurements of air velocity indicate that natural and traffic-induced winds contribute to the overall airflow inside the tunnel. A temperature data logger installed in the tunnel recorded temperature changes during the period of pandemic lockdown and subsequent recovery, spanning the spring and summer seasons. During the lockdown period, there was a relatively small increase in temperature along the tunnel, suggesting that vehicle heat dissipation is the primary factor contributing to temperature rise inside. Additionally, a method is proposed to predict the cross-sectional temperature of the tunnel using measured air velocities.

**Keywords:** ultra-long underwater tunnel; temperature distribution; ventilation; temperature control; on-site measurement



**Citation:** Gao, J.; Guo, W.; Ma, M.; Hou, Y.; Zhang, R.; Zeng, L.; Zhang, C.; Xu, Y.; Wei, X.; Cao, C. Study on Temperature Distribution along the Ultra-Long Underwater Tunnel: Based on the Long-Term Measured Results of the Shanghai Yangtze River Tunnel. *Buildings* **2023**, *13*, 1804. <https://doi.org/10.3390/buildings13071804>

Academic Editor: Lambros T. Doulou

Received: 19 June 2023

Revised: 8 July 2023

Accepted: 13 July 2023

Published: 15 July 2023



**Copyright:** © 2023 by the authors. Licensee MDPI, Basel, Switzerland. This article is an open access article distributed under the terms and conditions of the Creative Commons Attribution (CC BY) license (<https://creativecommons.org/licenses/by/4.0/>).

## 1. Introduction

Tunnels play a critical role in reducing traffic time and promoting economic growth in public transportation systems. Proper ventilation and temperature control are essential for ensuring their normal operation. Studies have shown that when cars pass through tunnels, they discharge polluted air and waste heat into the surrounding environment. Waste heat constitutes about 80% of the tunnel's total heat sources, with lighting, ventilation, and traffic control equipment contributing to the rest [1,2].

The heat generated by vehicles released into the tunnel can be transferred to the surrounding rock, which is driven forward by natural or mechanical ventilation through the shaft or tunnel exit, causing air temperature to rise inside the tunnel. In long tunnels with high traffic flow, the heat generated by vehicles can accumulate, causing the air temperature in the direction of tunnel ventilation to rise continuously. If the outdoor temperature is high, the temperature near the tunnel exit may exceed safety limits, leading to occupant thermal discomfort, unsafe tunnel operation, and damage to tunnel lining.

For instance, when the tunnel length exceeds 5 km at normal vehicle speed (80 km/h), occupants' exposure time in the tunnel can reach 6–10 min. The recommended exposure time and temperature in tunnels are 2.5 min above 40 °C [3]. Therefore, temperature increases tend to cause discomfort for passengers and maintenance personnel in tunnels and may exceed human tolerance. However, temperature rises in tunnels can lead to decreased engine efficiency and air-conditioning cooling capacity of vehicles and cause oil circuit faults. With the increasing proportion of electric vehicles, temperature rises in tunnels may also affect battery performance and safety, leading to traffic accidents.

In general, cooling measures must be applied once the air temperature in tunnels becomes too high. However, research on the temperature distribution inside tunnels typically focuses on the construction stage or fire scenario because of the significant impact of the internal temperature on the safety of construction workers, driver, and conductor [4–6]. Actual measurements and studies on the phenomenon of temperature rise throughout the tunnel are scarce. Therefore, understanding the reasons behind this phenomenon and its long-term impact on the operation of ultra-long tunnels is crucial. There is an urgent need for relevant actual measurement data support. The Shanghai Yangtze River Tunnel, an exceptionally long underwater tunnel, has been in operation for 14 years. Since the implementation of its monitoring system in 2018, a significant volume of data has been accumulated. However, there is currently a deficiency in conducting thorough analysis of this data, which is pivotal in comprehending the temperature and wind speed conditions inside the tunnel. Such analysis is crucial in guiding the daily ventilation operation of the tunnel.

The primary method used for cooling tunnels is increasing the ventilation rate, which involves the use of high-powered fans to enhance airflow and remove heat from the tunnel. However, in the case of exceptionally long tunnels, the required ventilation rate for temperature control can be much greater than that needed for pollutant control, leading to significant energy consumption and operational costs [7]. To address this issue, China's "Ventilation Design Rules for Highway Tunnels" (JTG/T D70/2-02-2014) have established guidelines for tunnel ventilation, specifying that the design ventilation velocity should not exceed 10 m/s for one-way traffic and 8 m/s for two-way traffic. These guidelines have proven effective in mitigating cooling and smoke extraction challenges by limiting the reliance on increasing ventilation rates in tunnels.

Current theories on tunnel ventilation primarily focus on sudden fires that may occur within tunnels [8–12]. Wan et al. [13] conducted a study on the performance of ceiling jets induced by dual, unequal, strong plumes in a naturally ventilated tunnel. The authors proposed models for maximum temperature and temperature decay profiles, which can be used to predict ceiling gas temperatures and the operating state of ceiling jets in tunnels. Yi et al. [14] analyzed the air inlet velocity and temperature distribution in an inclined tunnel with a single shaft under natural ventilation. Their findings suggest that the variation in fire source location, shaft height, and tunnel slope have a significant impact on the air inlet velocity. Collela et al. [15] developed a novel 3D coupled 1D modeling approach for ventilation flow in tunnels at ambient conditions (i.e., cold flow). Their work lays the foundation for coupling fire-induced flows and ventilation systems, where further complexities are introduced by the hot gas plume and smoke stratification. Oka et al. [16] investigated the ceiling-jet thickness and vertical distribution along a flat-ceilinged horizontal tunnel. They applied a cubic function and coordinate transformation to develop empirical formulae for the temperature and velocity distributions. Kim [17] utilized dynamic-grid numerical

simulations to examine the effects of vent shaft location on ventilation performance during fire emergencies in subway tunnels. Recently, Huang et al. [18] conducted an experimental investigation of temperature profiles with a downstream vehicle in a longitudinally ventilated tunnel. Their findings suggest that an ignited vehicle can result in a temperature hump and a larger high-temperature region downstream.

On the other hand, many works have been conducted on ventilation during the construction period of tunnels [19–23]. To address the high-temperature environmental hazards caused by concrete hydration heat release during tunnel construction, Wang [24] studied the heat generation mechanism of the heat source in the tunnel using theoretical analysis and numerical simulation and analyzed the temperature control in the tunnel under different ventilation wind speeds and ventilation temperatures. In order to evaluate the effect of ventilation on the thermal performance of tunnel lining ground heat exchangers during tunnel construction, thermal response field tests considering ventilation were performed in the Linchang tunnel. A 3D numerical model of tunnel lining GHEs was built and verified with the field monitoring data. Zhang et al. [25] proposed an air layer structure for controlling the thermal environment in high ground temperature tunnels and for meeting environmental requirements during tunnel construction. Thermal response field experiments on a mountain tunnel equipped with an air layer structure were conducted under tunnel ventilation and heating. The variations in air temperature inside the tunnel and thermal response characteristics of the surrounding rock under the condition of a tunnel with an air layer structure were analyzed. Lin et al. [26] innovatively established a high-temperature comprehensive control system for high geothermal tunnels, combining high-temperature treatment in the tunnel and high-temperature heat source insulation. The high-temperature comprehensive control system and cooling measures, including mechanical ventilation, are adopted based on on-site temperature monitoring so that the temperature in the tunnel can meet construction requirements.

The daily operation of tunnel ventilation systems is also crucial for maintaining safety. However, this operation differs from that during the fire and construction period [27]. In the Yangtze River Tunnel in Shanghai, a preliminary study found that the tunnel jet fans are often only opened briefly due to operating costs and noise [28], which can lead to local overheating caused by the accumulation of heat dissipation from tunnel vehicles. Guo et al. [29] reported that long tunnel ventilation systems in China require a significant investment for installation and have high energy consumption during operation. Unfortunately, even if they can be installed, they may not be affordable to operate. As a result, many ventilation systems have had to reduce their working time and service quality to cut down on expenses, and innovative and effective technologies are still lacking. Zhao et al. [30] have proposed a robust numerical method for modeling ventilation through long tunnels in high-temperature regions based on a 1D pipe model. They have pointed out that both ventilation velocity and time are crucial parameters that determine the air temperatures in the tunnel and surrounding rocks. Wang et al. [31] have investigated domestic and foreign tunnel ventilation design standards and have analyzed the impact of emission generation formula, base emission rates, and time factors on ventilation system design through a calculation example. Their research shows that the 2017 Shanghai Code and 2019 PIARC Ventilation Report consider the impact of NO<sub>2</sub> and non-emission particles on the demand for fresh air in tunnels, whereas the 2014 China Guidelines do not. Ciocanea et al. [32] have introduced the concept of modular ventilation and quantitatively studied the effects of air outlet placement and spacing on the tunnel temperature field. Chu et al. [33] have invented a GA-based fuzzy controller design for tunnel ventilation systems, which aims to maintain an adequate level of the CO pollutant concentration and visibility index (VI) while minimizing power consumption. Li's group [34,35] has conducted several significant works in tunnel ventilation, including testing the temperature, humidity, and air velocity based on the traffic flow statistics in an urban undersea road tunnel. They have also analyzed in detail the impact of the temperature difference between the outdoor air temperature during evening peak traffic flow and the ventilation design temperature at

14:00 on the ventilation rate. To control the temperature of undersea road tunnels, they have proposed a new method of determining the outdoor design temperature for summer ventilation. Furthermore, since there is still a lack of established efficient and energy-saving methods to control the cold air invasion of tunnels, they have used numerical simulation to determine that a new curved tunnel structure installed at the entrance of a tunnel can form an unpowered air curtain.

In summary, research on temperature distribution in tunnels is mainly focused on tunnel construction and fire scenarios. During normal tunnel operations, tunnel fans are usually not in operation due to energy consumption and noise issues associated with jet fans. However, the temperature inside the tunnel may gradually rise due to the accumulation of heat from vehicles, especially during summer when the tunnel is heavily congested and traffic airflow is low. At this time, the local temperature at the end of the tunnel may be very high, and relevant measured data are urgently needed to provide support for the time-sharing and staged operation of tunnel mechanical ventilation. This study was conducted against this background. We obtained temperature and wind speed data for the entire year of 2021 in the Shanghai Yangtze River Tunnel and conducted in-depth analysis. In addition, temperature, humidity, and wind speed measurements were conducted in the tunnel during winter and summer, and temperature data loggers were installed in the tunnel from February to June and in July to obtain a large amount of valuable measured data for the tunnel, which can provide data support for the routine maintenance of a large number of similar ultra-long underwater tunnels. Based on this, we propose a simple method to predict the cross-sectional temperature of the tunnel using measured air velocities. We also combine the tunnel's purification system with local air conditioning cooling to efficiently control the temperature rise in extremely high-temperature conditions at the exit of extra-long tunnels, while considering both economic and energy-saving factors.

## 2. Method

### 2.1. Tunnel Overview

The Shanghai Yangtze River Tunnel starts at the Luchongsu Interchange, passes through the south port waters of the Yangtze River, and ends at the Panyuan Road Interchange to the north. The total length of the route is 8955.26 m, with the main span of the river section being 7470 m. The net distance between the two single tubes is approximately 16 m, and the cross-sectional area of the tunnel is 177 m<sup>2</sup>. The outer diameter of a tube is 15 m, with an inner diameter of 13.7 m. The lane width is 3.75 m, the total width is 22.5 m, and the maximum depth is 55 m. The road is a two-way six-lane highway, designed for a speed of 80 km/h. The cross-sectional view of the tunnel is shown in Figure 1.

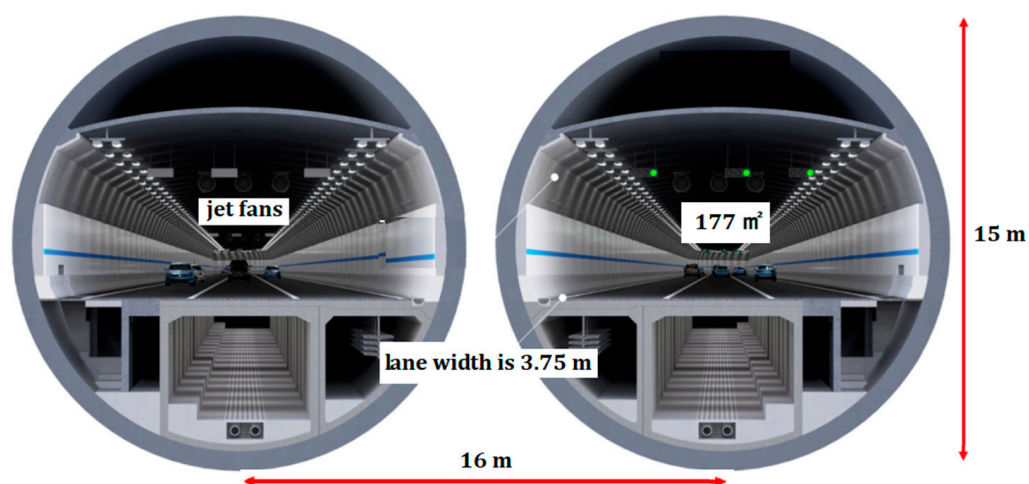


Figure 1. The cross-sectional view of the Shanghai Yangtze River tunnel.

The tunnel consists of a surface road, an underwater tunnel section, and various interchanges. The main section of the tunnel's horizontal road is shaped like an "S" and is arranged in a northeast to southwest direction. The main river-crossing section of the tunnel consists of a double-line circular tunnel, and the tunnel lining is made of reinforced concrete pipe sections. The tunnel is divided into three levels: the upper level is the smoke exhaust duct, the middle level is the three-lane highway lane, which does not have an emergency parking lane, and the lower level is reserved for rail space, escape routes, and equipment channels. Stairwells for evacuation are located between the middle and lower levels.

The cross-sectional layout of the circular tunnel can be divided into three levels: the top of the tunnel is for smoke exhaust fans, smoke exhaust ports, and jet fans; the middle section is for the three-lane highway, with variable message signs, lighting fixtures, emergency broadcasts, cameras, water spray nozzles, and other equipment above the lanes; and below the lanes are reserved for rail traffic channels. Three to four jet fans are arranged in the same longitudinal position, evenly arranged along the way, totaling 107 sets. The Shanghai Yangtze River Tunnel has wind towers on both Pudong and Changxing Islands, which contain exhaust fans and axial flow smoke exhaust fans. During normal and obstructed traffic conditions, the polluted air inside the tunnel is discharged at high altitude to reduce environmental pollution caused by the tunnel's exit. During fire conditions, smoke exhaust fans are activated, and smoke inside the tunnel is discharged and controlled through the smoke exhaust duct on the arch, which helps with evacuation and rescue.

## 2.2. Measuring Process

A large amount of recorded data on air velocity and temperature was retrieved and processed through cooperation with the management company of the Shanghai Yangtze River Tunnel. The company stated that the sensors (temperature, air velocity, etc.) near the upstream exit of the tunnel were regularly calibrated, and the data were reliable. Then, the actual measurements of the internal environmental parameters of the Shanghai Yangtze River Tunnel include winter and summer testing. The winter testing was conducted from 23:00 on 23 February 2022, to 1:00 on 24 February 2022, and the summer testing was conducted from 23:00 on 12 July 2022, to 2:00 on 13 July 2022. During the tunnel testing process, two out of three lanes were open for normal traffic while the tunnel operator provided us with a roller compactor to close off one lane for testing. The traffic flow inside the tunnel was not affected at that time. 21 measuring points were arranged longitudinally along the tunnel, mainly in areas such as emergency and connecting passages that were convenient for fixing instruments (the on-site measurement photos are shown as in Figure 2). The wall temperature of the tunnel was measured using an infrared thermometer (model FLIR TG65, accuracy  $\pm 1.5$  °C, resolution 0.1 °C, measurement range  $-25$ – $380$  °C) at each measuring point. The air velocity was measured using a hot wire anemometer (model WFWZY-1, accuracy  $\pm 0.05$  m/s, resolution 0.01 m/s, measurement range 0.05–30 m/s), and the temperature and humidity were measured using an temperature and humidity meter (temperature accuracy 1%, temperature resolution 0.1 °C, measurement range  $-40$ – $100$  °C; humidity accuracy 3 RH, humidity resolution 0.1 RH, measurement range 0–100% RH). A temperature data logger (model WZY-1, accuracy  $\pm 0.3$  °C, resolution 0.1 °C, measurement range  $-20$ – $80$  °C) was installed to record the air temperature at each measuring point for a period of time (the instruments used for winter testing were retrieved on June 9, and those used for summer testing were retrieved on 1 August). The outdoor temperature, humidity, and air velocity on the day of the actual measurements were obtained directly from on-site measurements, and the outdoor temperature data corresponding to the temperature data logger were obtained by retrieving temperature data from two meteorological stations near the entrance and exit of the tunnel.

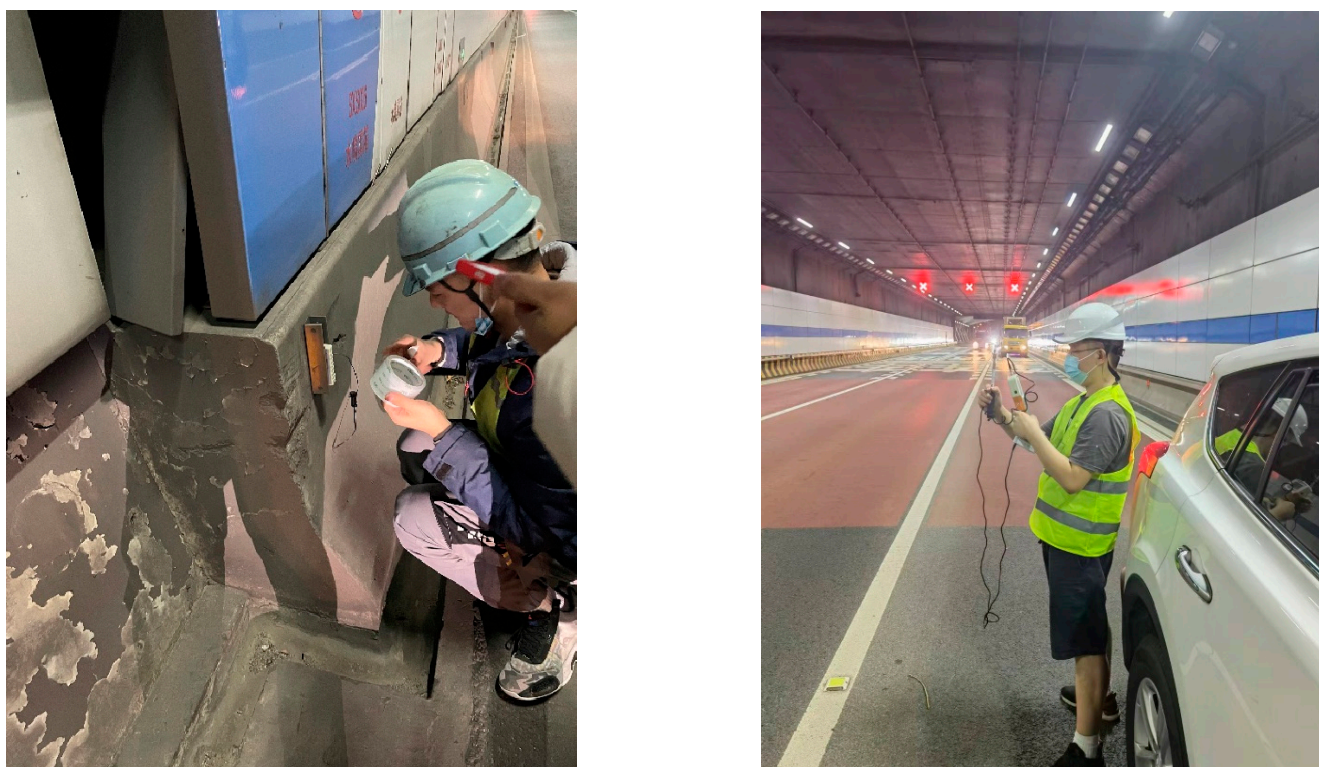


**Figure 2.** Site pictures for winter and summer test.

### 3. Results

#### 3.1. Operation Monitoring Data

Due to our primary focus on the temperature distribution at the tunnel exit location (approximate worst-case measurement point), we analyzed the data provided by the tunnel management company only for the entire year of 2021 at that point. We retrieved and organized several relevant data from the database of the Yangtze River Tunnel and extracted monitoring data from the typical periods at the tunnel exit measurement point. As 8:00, 17:00, and 18:00 correspond to the peak commuting time of Shanghai's morning and evening rush hours, we organized the data for these time periods and also selected the data from 15:00, a time with lower traffic volume, as supplementary. Since the upstream exit of the tunnel is close to Chongming District, we also retrieved the hourly historical temperature data for Chongming District for the entire year of 2021 as a comparison. We hope to obtain the relationship between the temperature distribution at the tunnel exit and the annual temperature distribution of the region by analyzing the data and clarify the impact of traffic volume on the cumulative effect of tunnel temperature. The monitoring data of the tunnel exit temperature at 8:00, 15:00, 17:00, and 18:00 in 2021 for the entire year are shown in Figure 3, and the corresponding historical temperature data for Chongming District at 8:00, 15:00, 17:00, and 18:00 in 2021 are also shown in Figure 3.

The temperature of tunnel exit is mainly affected by the superimposition of outdoor temperature and traffic volume. Overall, the temperature distribution near the exit of the Yangtze River Tunnel exhibits a hot summer and cold winter pattern throughout the year, with the lowest temperature occurring in January and the highest temperature occurring in July and August (the average temperature in August is higher than in July), indicating that the tunnel temperature is greatly affected by fluctuations in outdoor temperature. Although there is a large traffic volume at 8:00, the monitoring temperature throughout the year is lower due to the lower outdoor temperature than in the afternoon. The traffic volume and outdoor temperature are both higher in the afternoon from 17:00 and 18:00, so the monitoring temperature peak occurs at this time of day throughout the year. Figure 3c

shows that the highest temperature in the tunnel in 2021 occurred at 17:00 on 25 August, reaching 39.74 °C.

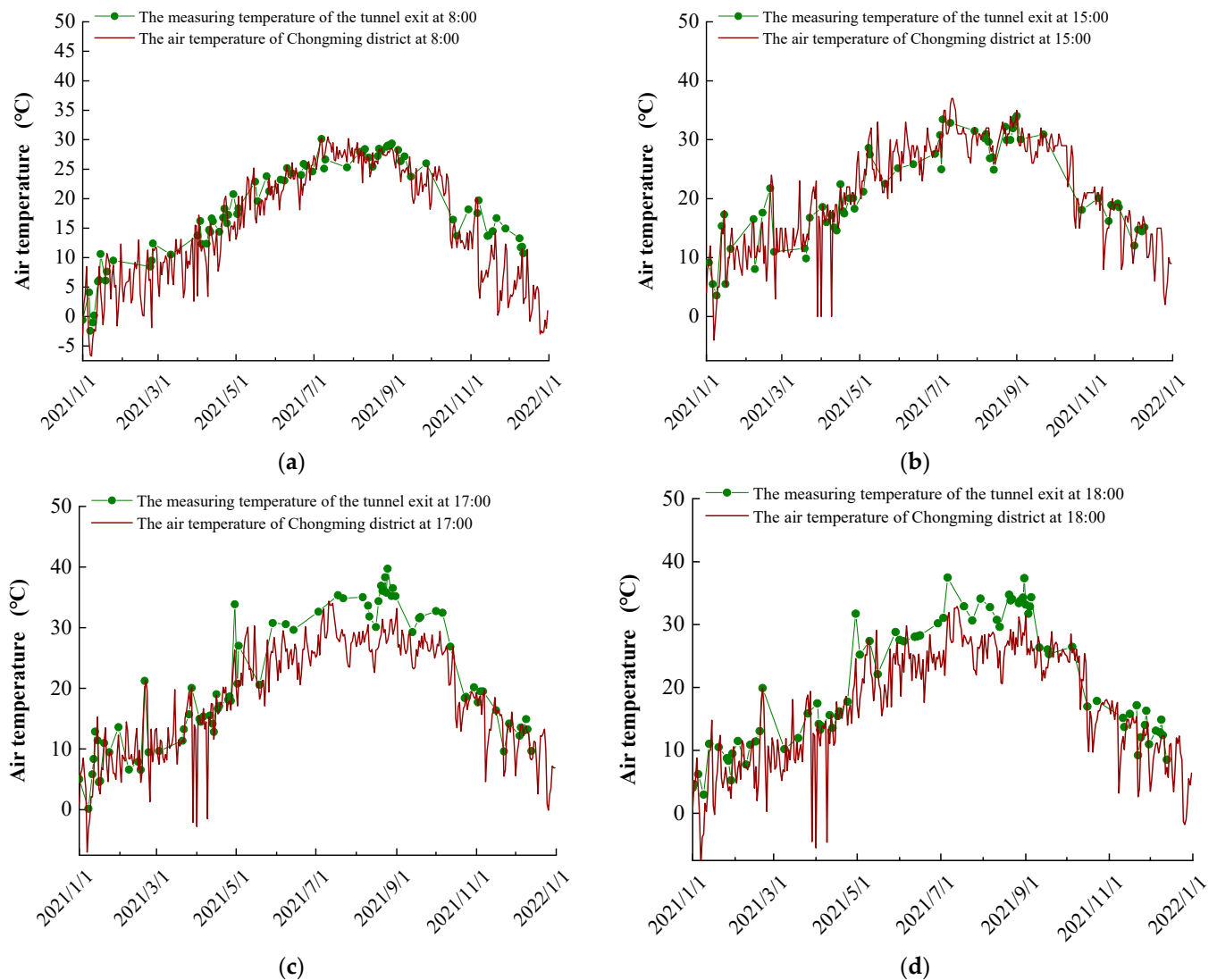


**Figure 3.** Data for temperature monitoring at the tunnel exit and in Chongming district during certain periods: (a) Data at 8:00; (b) Data at 15:00; (c) Data at 17:00; (d) Data at 18:00.

When comparing and analyzing the daily hourly temperatures in Chongming district that year, it was found in Figure 3a that the temperature difference between the temperature at 8 am in the summer and the tunnel temperature was relatively small. This is because the tunnel air temperature in the summer is affected by the heat exchange of the lining, the external temperature, and the heat dissipation of the cars. The lining directly exchanges heat with the soil at a lower temperature in the Yangtze River, resulting in a lower temperature in the tunnel air, which leads to a certain degree of temperature drop. At the same time, the temperature at 8:00 is generally 2–3 °C lower than the average temperature of the day, so the temperature at the tunnel exit is relatively close to the temperature in Chongming district in the summer at 8:00. After entering the winter season, the temperature at the tunnel exit during this time period is significantly higher than the temperature in Chongming district. This is because the tunnel has a thermal insulation effect in the winter, and the heat dissipation from the cars in morning rush gradually converges towards the tunnel exit due to the effects of traffic and natural wind, forming a heat accumulation zone near the exit, which raises the air temperature. At the same time, due to the low temperature at 8:00, the

temperature difference between the two is even more obvious. From Figure 3b, it can be seen that the temperature at the tunnel exit at 15:00 is relatively close to the temperature in Chongming district, and the temperature difference between the two in the winter at 8 am is smaller than in the afternoon at 15:00. This is because the traffic volume is smaller in the afternoon (before 17:00), and the tunnel heat accumulation caused by car heat dissipation is not significant, so the temperature at the tunnel exit rises limitedly. In addition, the temperature at 3 pm usually corresponds to the highest temperature of the day, so the temperature difference between the tunnel exit and the temperature in Chongming district is relatively small during this period. From Figure 3,d, it can be seen that 17:00 and 18:00 is the peak period of traffic volume in the evening rush hour, and there is a large amount of car heat dissipation, leading to a significant heat accumulation effect at the tunnel exit, especially in the winter and summer seasons. Therefore, the temperature at the tunnel exit at 17:00 to 18:00 is about 3–8 °C higher than the temperature in Chongming district, and the temperature difference is greater in summer than in winter.

We have obtained the hourly air velocity data at the exit of the tunnel in October 2021. The results show that although the Yangtze River Tunnel seldom turns on the jet ventilation system to save operating costs and reduce the impact of fan noise on residents, the natural wind and traffic flow inside the tunnel can still form an air velocity of around 2–6 m/s. The air velocity distribution is generally random, but the time when the monitored air velocity is low is mainly during the morning and evening rush hours. This is because traffic congestion leads to a decrease in traffic wind speed, which in turn causes a decrease in the tunnel exit wind speed (the vector sum of traffic and natural wind). Compared with the average air velocity in Chongming District in October 2021 (not considering the wind direction), the tunnel exit air velocity is significantly higher, indicating that traffic wind inside the tunnel contributes significantly to the monitored air velocity. When traffic is smooth, the air velocity inside the tunnel can reach 6 m/s, and the contribution rate of traffic wind exceeds 50%. From Figure 4, it can also be seen that the air velocity at the tunnel exit during peak traffic hours is close to the hourly average wind speed in Chongming District, indicating that the traffic-induced wind at the tunnel exit tends to be zero at this time, and natural wind is dominant.

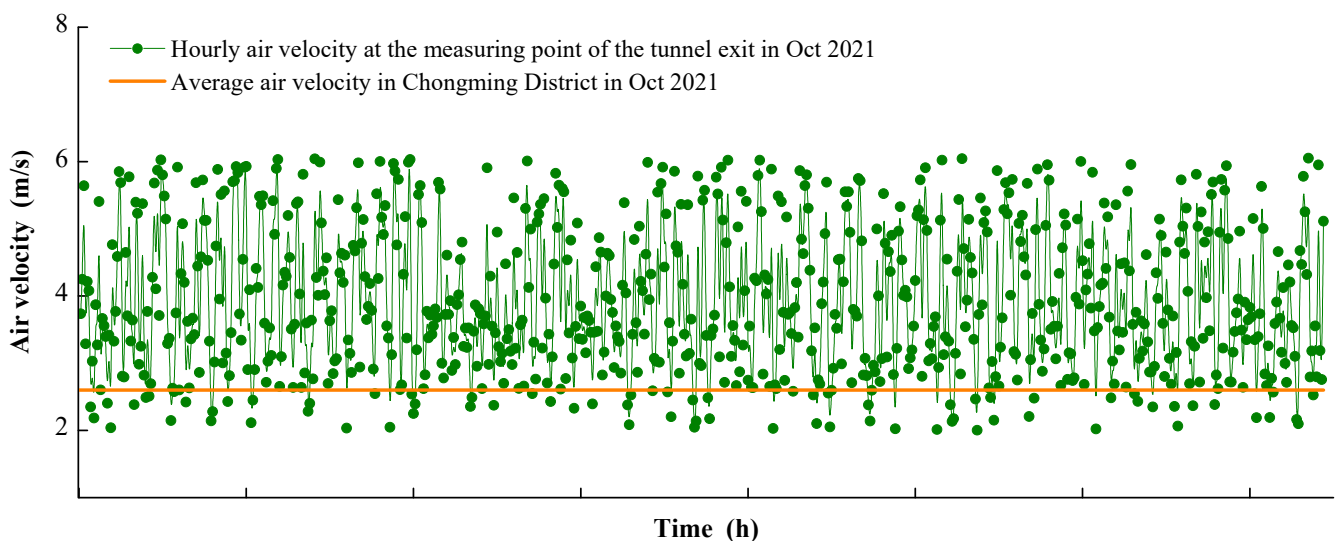


**Figure 4.** Hourly data for air velocity monitoring at the tunnel exit and in Chongming district during October 2021.

### 3.2. Field Measurement Data

During the winter and summer measurements, we tested the ground wall temperature, upper/left/right lining wall temperature at 21 measurement points. We also measured the air velocity, temperature, and humidity at each measurement point. After data processing,

the measuring results of the winter and summer air velocity, temperature, and humidity are shown in the Figure 5.

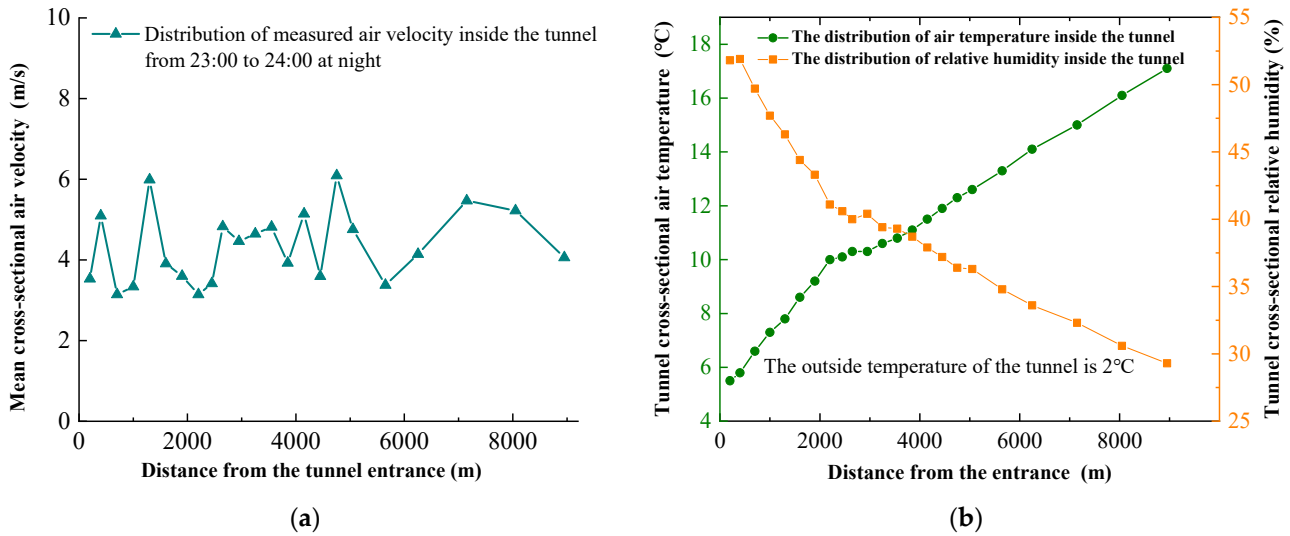


Figure 5. Results depict (a) measured winter air velocity and (b) air temperature and humidity in the tunnel.

According to the test results, in winter, the air velocity inside the tunnel fluctuates between 3–6 m/s, mostly around 5 m/s. At this time, the tunnel mechanical ventilation system was not turned on, so the air velocity was mainly affected by the traffic flow. The time of measurement was from 23:00 to 24:00, during which the traffic volume was relatively low. It can be predicted that if the traffic volume increases and there is no congestion and the vehicle speed is normal, the traffic-induced air velocity will further increase, but the increase will be limited. As shown in Figure 6b, the air temperature inside the tunnel increases from the entrance to the exit, which is consistent with the accumulation of heat effect. At the same time, the relative humidity of the air inside the tunnel gradually decreases along the way, mainly due to the increase in the saturated vapor pressure caused by the increase in air temperature. Under the condition where the vehicles almost do not release or absorb moisture, the relative humidity gradually decreases along the way.

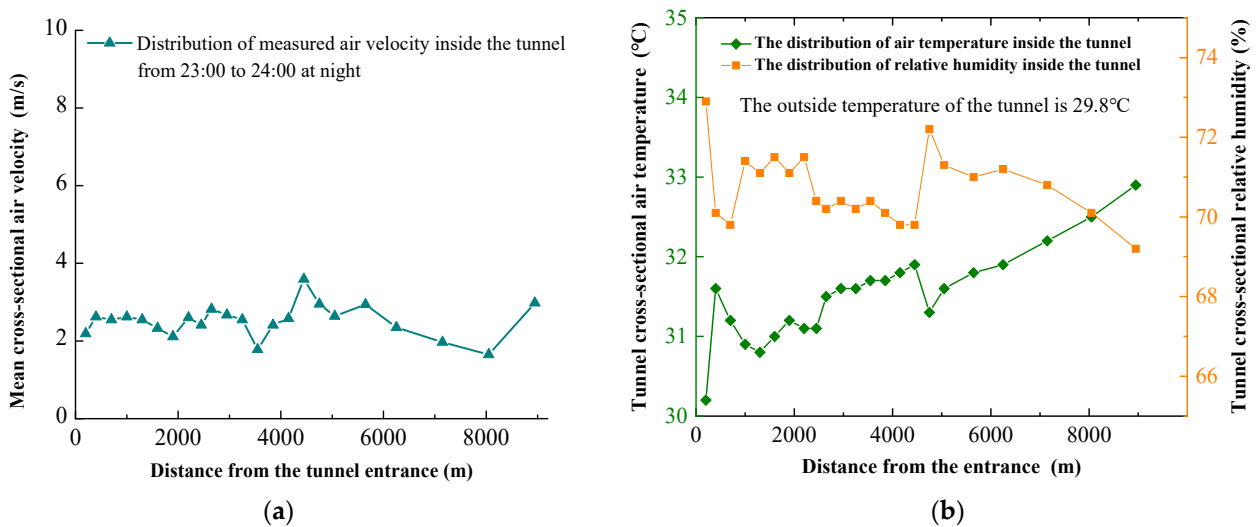


Figure 6. Results depict (a) measured summer air velocity and (b) air temperature and humidity in the tunnel.

Different from the results in winter, the air velocity inside the tunnel fluctuates between 2–3 m/s in summer, mostly around 2 m/s. Compared with the winter test results, the air velocity inside the tunnel is significantly lower in summer. We found that the natural wind speed outside the Chongming Island Tunnel in Shanghai on the day of the summer test was small, at 0.27 m/s, while the natural wind speed outside the Chongming Island Tunnel in Shanghai on the day of the winter test was large, at 2.8 m/s. The traffic volume during the same time period in both seasons was not much different, so it is speculated that the difference in the test results of air velocity between winter and summer is mainly influenced by the natural wind speed inside the tunnel. As shown in the Figure 6, the air temperature inside the tunnel increases from the entrance to the exit, consistent with the accumulation of heat effect (rising from 30.2 °C to 32.9 °C), but compared with the temperature rise in the same period in winter (rising from 5.8 °C to 17.1 °C in Figure 5), the temperature rise in summer (2.7 °C) is significantly lower. It has been found that in winter, the enclosing structure of an underwater tunnel plays a role in insulating the tunnel, and the enclosing structure acts as a heat storage unit, causing a significant increase in temperature along the tunnel. In summer, however, the enclosing structure of an underwater tunnel comes into direct contact with the outside water and sediment (which have temperatures significantly lower than outdoor air), and the enclosing structure acts as a cold storage unit, causing the heat dissipation of the cars to be transferred to the tunnel enclosure, resulting in an overall smaller temperature increase along the tunnel. These phenomena are similar to the phenomenon of cool summers and warm winters in caves. With regard to the relative humidity inside the tunnel, the overall relative humidity of the air gradually decreases along the tunnel in both winter and summer. This is mainly due to the increase in air temperature causing an increase in the saturated vapor pressure, resulting in a gradual decrease in relative humidity when there is almost no moisture exchange between the vehicles and the tunnel walls. It should be noted that the difference in the decrease in relative humidity between winter and summer is mainly due to the temperature difference.

We then conducted a statistical analysis of the temperatures of various tunnel walls in winter, and the results are shown in Figure 7 below.

In winter, the temperature distribution of all tested walls of the tunnel section is similar, with the temperature increasing from 0 °C at the tunnel entrance to about 15 °C at the exit. The temperature rise near the exit tends to level off, while in the middle section of the tunnel, the temperature rises almost linearly. At the same time, the wall temperature in winter is slightly lower than the air temperature, indicating that the lining of the tunnel has a good insulation effect on the tunnel. The heat emitted by the cars during the driving process has evenly heated the tunnel, and some of the heat is brought to the back half of the tunnel by the traffic ventilation, making the overall temperature rise of the tunnel walls more significant.

The statistical results of the wall temperature test in summer are shown in the Figure 8. In summer, the temperature of the walls on both sides of the tunnel section is about 1–2 °C lower than the air temperature inside the tunnel. From the entrance to the exit, the temperature of each wall gradually increases, but the increase is only around 3 °C. The temperature rise inside the tunnel is not significant, and in some points along the tunnel, there are even cases of temperature decrease. This is because the tunnel lining directly exchanges heat with the surrounding soil and water, forming a natural cold source that continues to cool the tunnel. It can be predicted that when the traffic volume increases, especially in traffic jams, the temperature rise along the tunnel will further increase. If the outdoor temperature in summer exceeds 35 °C, the tunnel's heat accumulation effect may cause the temperature near the exit of the tunnel to exceed the limit of 40 °C.

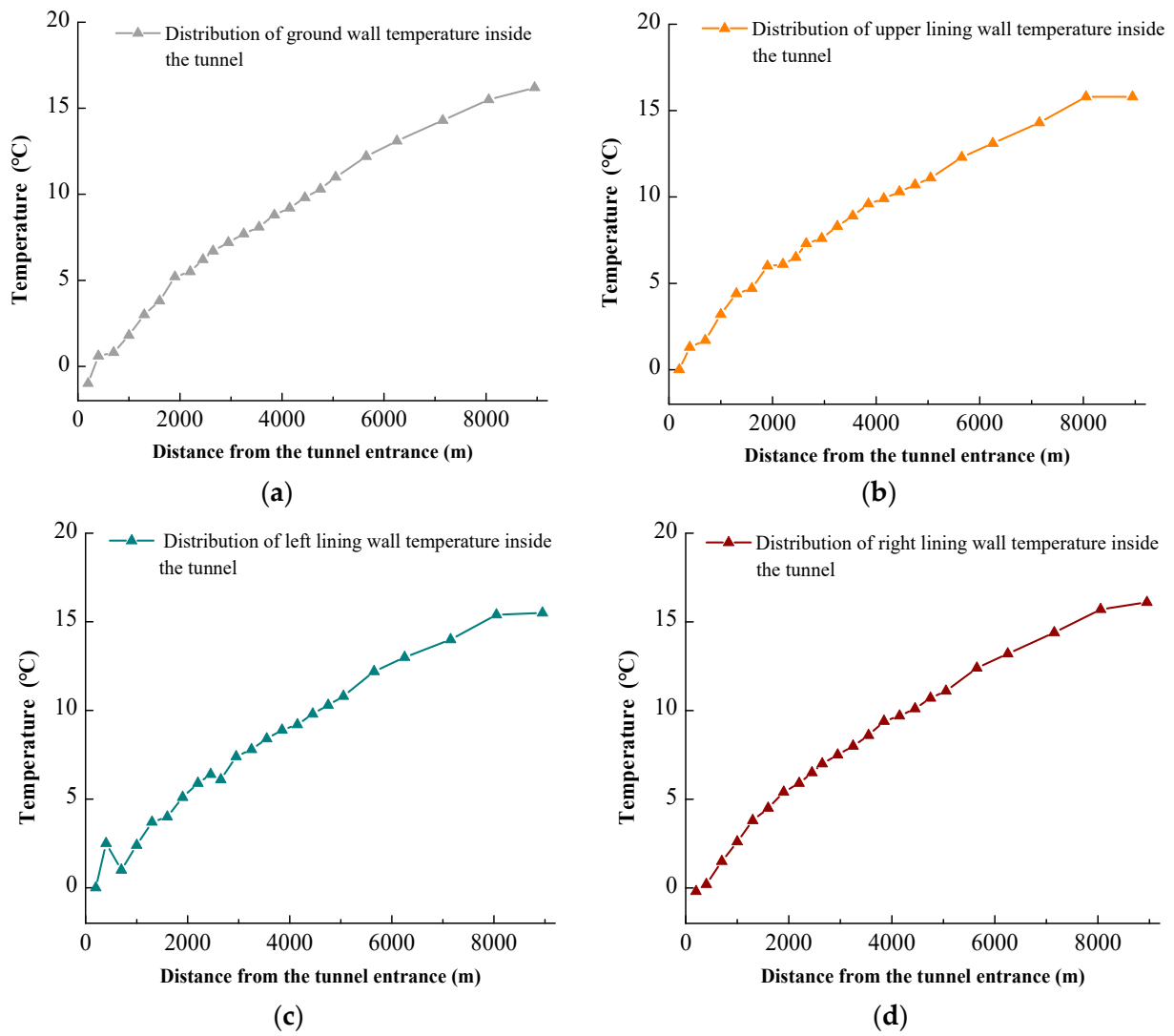


Figure 7. Measured results of tunnel lining wall temperature in winter: (a) Distribution of ground wall; (b) Distribution of upper wall; (c) Distribution of left wall; (d) Distribution of right wall.

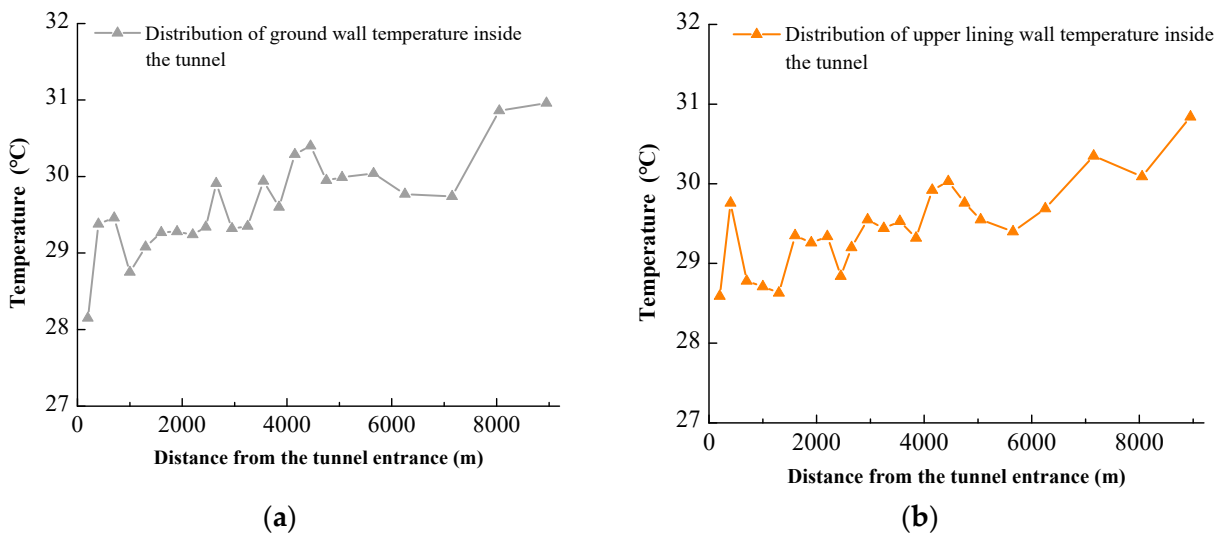
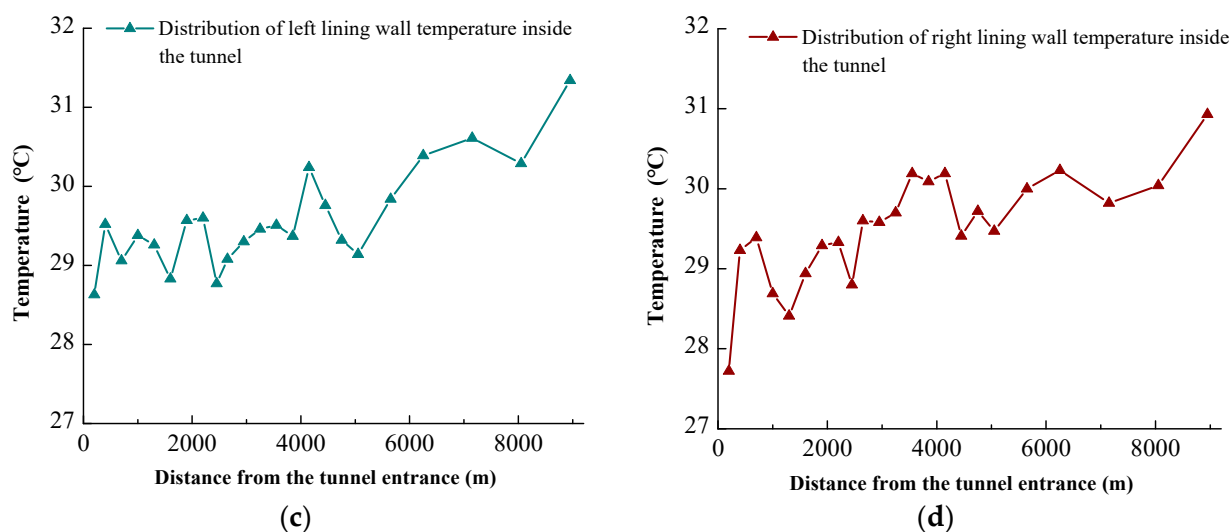


Figure 8. Cont.



**Figure 8.** Measured results of tunnel lining wall temperature in summer: (a) Distribution of ground wall; (b) Distribution of upper wall; (c) Distribution of left wall; (d) Distribution of right wall.

### 3.3. Long-Term Measurement Data

On 23 February 2022, we deployed 21 temperature data loggers in the Shanghai Yangtze River Tunnel. Due to the city's lockdown during the COVID-19 outbreak in 2022, the instruments were retrieved on June 9 when they still had power. Firstly, we organized the data from February 23 to June 8. As the data logger recorded the temperature every 10 min, we calculated the daily average temperature of each measurement point for ease of graphical analysis. We also kept track of the highest temperature recorded at each measurement point on the same day. Based on Figure 9, it can be observed that the cumulative temperature effect inside the tunnel decreases as the outdoor temperature increases. During winter, the temperature rise from the entrance to the exit of the tunnel can reach up to 12 °C, while in spring, it is generally reduced to below 5 °C, with some days having a temperature rise of only 2–3 °C. It was also found that the temperature inside the tunnel in winter is significantly higher than the daily average temperature in the Chongming District. However, in spring, the temperature inside the tunnel at sometimes is even lower than the outside air temperature, indicating that the tunnel has a thermal insulation effect in winter. After spring and summer, the heat exchange between the tunnel enclosure structure and the outside water and soil reduces the temperature of the inner wall of the tunnel, indirectly lowering the air temperature inside the tunnel. Additionally, Figure 9 shows that during the period of epidemic prevention and control, the temperature rise along the tunnel decreased to some extent. This was due to the gradual increase in temperature on the one hand, and the decrease in traffic flow and heat dissipation from vehicles caused by the control measures on the other hand, resulting in a less obvious temperature rise along the tunnel caused by the heat dissipation of vehicles and traffic ventilation effect.

To obtain the temperature distribution in the Shanghai Yangtze River Tunnel during summer, temperature recorders were installed again on the night of July 12th, and the instruments were retrieved on 1 August. During this period, the instruments worked normally, and the data from 12 July to 1 August were further processed using the same method as in winter. As shown in Figure 10, the temperature rise along the tunnel in summer is generally between 2–4 °C, which is consistent with the on-site measured data on the night of 12 July. If the monitoring data of the highest temperature inside the tunnel on the same day is further combined (5 min interval data, only briefly appearing during the afternoon rush hour), the maximum temperature rise along the tunnel is about 5.5 °C. The highest temperature inside the tunnel occurred on 14 July, which is the day with the highest daily average temperature in Shanghai in July, reaching 39 °C. As the ventilation

system of the Shanghai Yangtze River Tunnel was not operating during its operation in July, it can be anticipated that the measured temperature will be further reduced when the ventilation system is turned on.

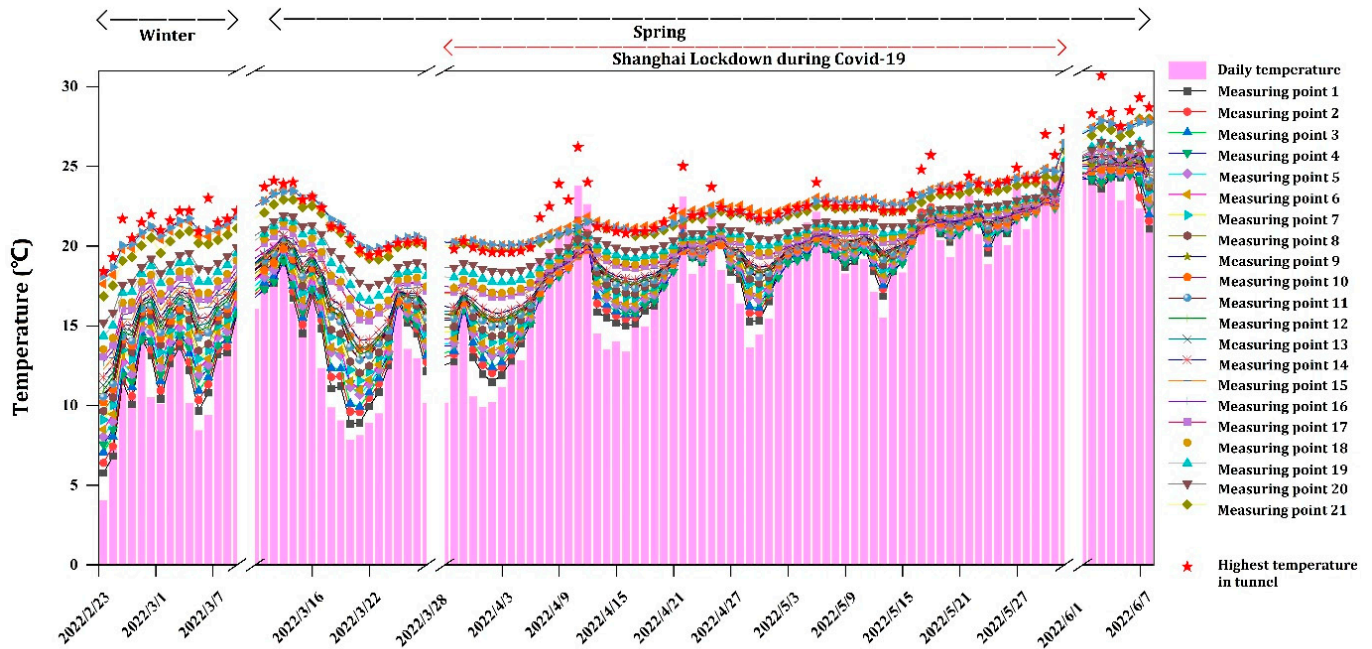


Figure 9. Recorded results of tunnel temperature data logger in winter and spring.

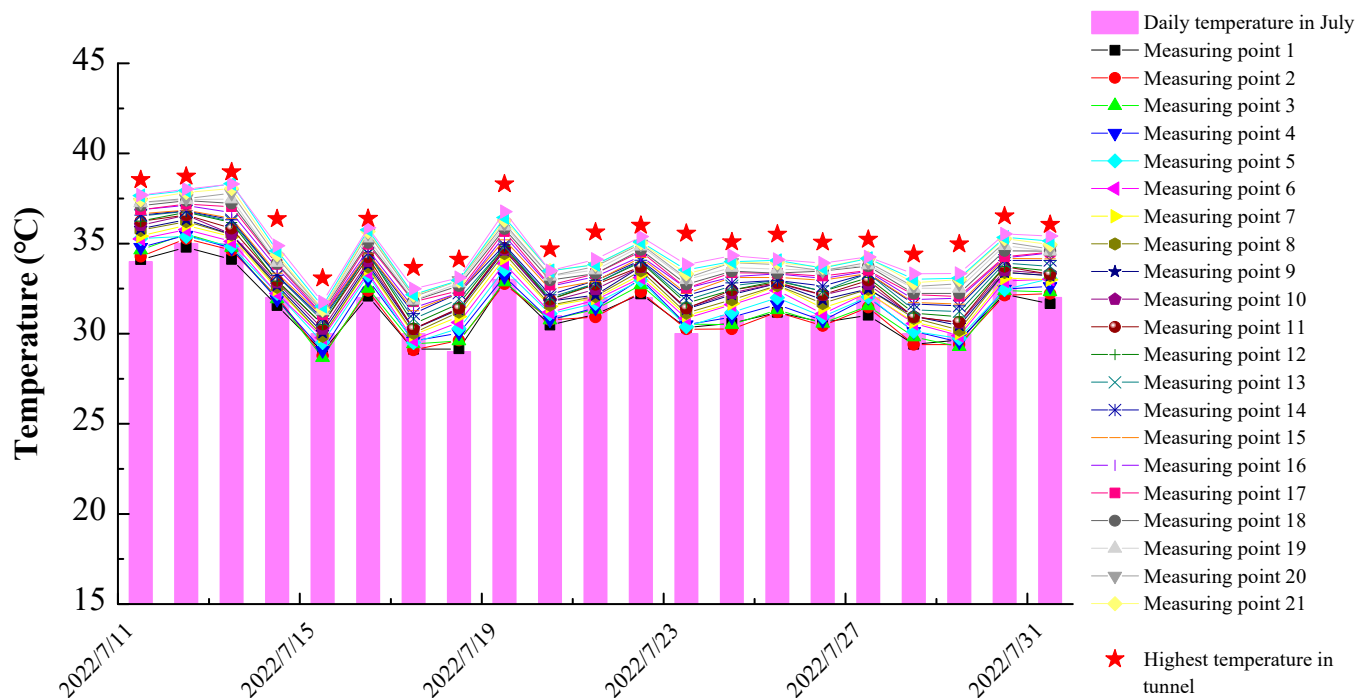
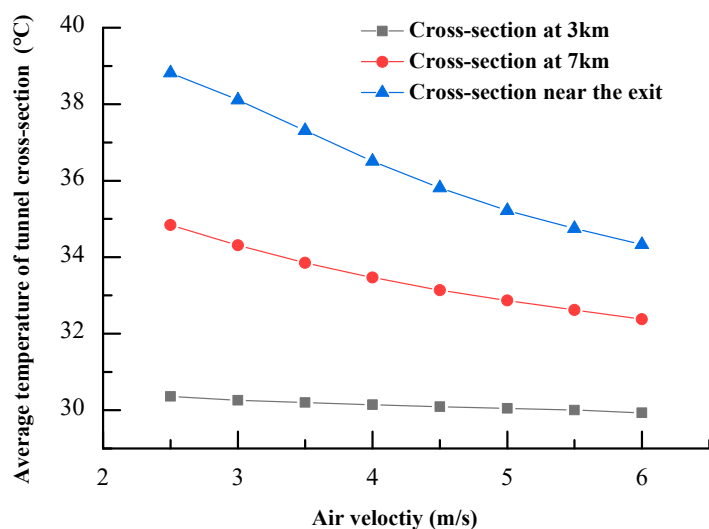


Figure 10. Recorded results of tunnel temperature data logger in summer.

#### 4. Discussion

After compiling the data provided by the tunnel operator for the year 2021, we noticed a correlation between the measured wind speed and the temperature inside the tunnel (Figure 11 was generated by fitting the data based on wind speed and temperature information provided by the tunnel operator for the year 2021). Specifically, we found

that higher wind speeds at measurement points inside the tunnel corresponded with lower temperatures at those points, assuming the temperature outside the tunnel remained constant at a given time. This correlation was most pronounced at measurement points closer to the tunnel exit, where the convective heat transfer effect was enhanced due to the higher temperature of the air in that area. By fitting different curves to the relationship between temperature and wind speed in different sections of the tunnel, we can predict the temperature at a given point as long as we know the wind speed, and vice versa. Using this information, we can turn on the jet fan to create a predictable change in temperature with wind speed, extending the curve we have fitted. This provides a more straightforward method for predicting temperature changes in different sections of the tunnel and can be useful in practical applications.



**Figure 11.** The relationship between measured air velocity and temperature at different cross-section measuring points inside the tunnel in summer.

With the increase of traffic volume in recent years, the congestion of Shanghai Yangtze River Tunnel during peak hours has become increasingly severe, especially during weekends and holidays. Due to long-term traffic congestion, commuting time from Pudong to Chongming may last for several hours. It can be foreseen that in the high temperature weather of summer, due to the large amount of heat emitted by car engines and refrigeration, and the extremely small traffic wind during congestion, the phenomenon of heat accumulation in the tunnel will intensify. Under such extreme unfavorable working conditions, based on the above measured results, it can be predicted that the area where the temperature in the tunnel exceeds the limit will be close to the tunnel exit, and the time when this most unfavorable working condition occurs is extremely limited. For China's newly-built super-long tunnels such as the Haitai Tunnel, their length is longer than the Shanghai Yangtze River Tunnel and their designed traffic volume is greater. Under the premise of extremely small traffic winds caused by extreme congestion, conventional tunnel jet ventilation alone is difficult to meet the local temperature control requirements near the tunnel's exit. If high-temperature areas in similar tunnels that have already been built can be identified through long-term measurements, the cooling capacity required for local overheating areas can be predicted by combining numerical simulation results of the tunnel temperature field. Local air conditioning and refrigeration facilities can be installed on sections of the tunnel where there is a risk of overheating.

Based on the principles of conservation of energy and mass, the cooling capacity required for local cooling in the tunnel can be calculated using the following formula:

$$Q = (T_{\text{out}} - T_0) \cdot \rho \cdot c_p \cdot v \cdot A \quad (1)$$

where  $Q$  represents the required cooling capacity of the cooling equipment,  $W$ .  $T_{\text{out}}$  represents the average temperature at the tunnel exit section,  $^{\circ}\text{C}$ .  $T_0$  represents the temperature limit of the tunnel,  $^{\circ}\text{C}$ .  $\rho$  represents the air density,  $\text{kg}/\text{m}^3$ .  $c_p$  represents the specific heat capacity of air at constant pressure,  $\text{J}/(\text{kg}\cdot^{\circ}\text{C})$ .  $v$  stands for air velocity in the tunnel,  $\text{m}/\text{s}$ .  $A$  represents the cross-sectional area of the tunnel,  $\text{m}^2$ .

The fan of the air purification system (previously designed and installed) at the end of the tunnel can be used to deliver the cooled air to the overheating area in a short period of time. This approach is expected to save initial investment and operating costs while ensuring that the local temperature does not exceed the limit.

## 5. Conclusions

In conclusion, proper ventilation and temperature control are crucial for the normal operation of tunnels, especially in long tunnels with high traffic flow. The heat generated by vehicles released into the tunnel can cause the air temperature to rise, leading to discomfort for occupants, low vehicle performance, and potential damage to the tunnel infrastructure.

Research on temperature distribution in tunnels has primarily focused on tunnel construction and fire scenarios, with limited studies on temperature rise during normal tunnel operations. The accumulation of heat from vehicles, particularly during congested periods, can result in high temperatures at the tunnel exit. Actual measurement data are urgently needed to support the time-sharing and staged operation of tunnel mechanical ventilation and routine maintenance of similar ultra-long tunnels.

This study, conducted in the Shanghai Yangtze River Tunnel, provides valuable measured data for understanding temperature and air velocity patterns throughout the year. The analysis reveals that the temperature at the tunnel exit is influenced by outdoor temperature and traffic volume, with higher temperatures observed during peak traffic hours. This work also demonstrates that the air temperature rises by approximately  $11\text{ }^{\circ}\text{C}$  from the tunnel entrance to the exit, while the wall temperature increases by about  $15\text{ }^{\circ}\text{C}$ . In contrast, during the summer, the air temperature only increases by  $2.7\text{ }^{\circ}\text{C}$ , and the wall temperature increases by around  $3\text{ }^{\circ}\text{C}$ . As a result, the humidity decreases along the tunnel, and this decrease is correlated with the magnitude of the temperature increase. Furthermore, measurements of air velocity indicate that both natural and traffic-induced winds contribute to the overall airflow inside the tunnel. A temperature data logger installed in the tunnel recorded temperature changes during the period of pandemic lockdown and subsequent recovery, spanning the spring and summer seasons. During the lockdown period, there was a relatively small increase in temperature along the tunnel, suggesting that vehicle heat dissipation is the primary factor contributing to the temperature rise inside.

Based on the findings, a simple method is proposed to predict the cross-sectional temperature of the tunnel using measured air velocity. The study suggests integrating the tunnel's end ventilation and purification system with local air conditioning cooling as an efficient approach to controlling temperature rise in extremely high-temperature conditions of extra-long tunnels, while considering economic and energy-saving factors.

In summary, understanding temperature distribution in tunnels and implementing effective cooling strategies are essential for ensuring safe and comfortable tunnel operations. Further research and data collection are needed to improve the understanding of temperature dynamics in tunnels and support the development of efficient and sustainable cooling solutions.

**Author Contributions:** Conceptualization, J.G. and L.Z.; Methodology, W.G., R.Z. and L.Z.; Validation, M.M., C.Z., Y.X., X.W. and C.C.; Investigation, W.G., M.M. and Y.H.; Data curation, W.G.; Writing—original draft, L.Z.; Writing—review & editing, J.G. and R.Z. All authors have read and agreed to the published version of the manuscript.

**Funding:** This study was funded by the Hai Tai Cross-River Tunnel Project (Led by Jiangsu Provincial Department of Transportation, Grant number: kh0100020221702).

**Data Availability Statement:** The data presented in this study are available on request from the corresponding author.

**Acknowledgments:** The authors also would like to express their gratitude to the Shanghai Yangtze River Tunnel and Bridge Control Center for providing the tunnel monitoring data.

**Conflicts of Interest:** The authors declare no conflict of interest.

## References

1. Wang, M. An overview of development of railways, tunnels and underground works in China. *Tunn. Undergr. Space Technol.* **2010**, *30*, 351–364. [[CrossRef](#)]
2. Lai, J.; Wang, X.; Qiu, J.; Zhang, G.; Chen, J.; Xie, Y.; Luo, Y. A state-of-the-art review of sustainable energy-based freeze proof technology for cold-region tunnels in China. *Tunn. Undergr. Space Technol.* **2018**, *82*, 3554–3569. [[CrossRef](#)]
3. Yasuda, N.; Tsukada, K.; Asakura, T. Field measurements of environmental parameter and pollutant dispersion in urban undersea road tunnel. *Tunn. Undergr. Space Technol.* **2019**, *149*, 100–108. [[CrossRef](#)]
4. Srinavin, K.; Mohamed, S. Thermal environment and construction workers' productivity: Some evidence from Thailand. *Tunn. Undergr. Space Technol.* **2003**, *38*, 339–345. [[CrossRef](#)]
5. Yunpeng, H.; Mingnian, W.; Qiling, W.; Dagang, L.; Jianjun, T. Field test of thermal environment and thermal adaptation of workers in high geothermal tunnel. *Tunn. Undergr. Space Technol.* **2019**, *160*, 106174. [[CrossRef](#)]
6. Tang, F.; He, Q.; Shi, Q. Experimental study on thermal smoke layer thickness with various upstream blockage–fire distances in a longitudinally ventilated tunnel. *Tunn. Undergr. Space Technol.* **2017**, *170*, 141–148. [[CrossRef](#)]
7. Shi, Y. Study on Calculation Method of Natural Wind and Energy Saving Ventilation Technology on Tunnel. Ph.D. Dissertation, Southwest Jiaotong University, Chengdu, China, 2011.
8. Cong, W.; He, K.; Yang, H.; Shi, L.; Cheng, X. Experimental study on temperature characteristics in a subway train carriage with lateral openings in a longitudinally ventilated tunnel. *Tunn. Undergr. Space Technol.* **2023**, *131*, 104814. [[CrossRef](#)]
9. Yan, J.; Chen, G.; Liu, C.; Tang, L.; Chen, Q. Maximum smoke temperature beneath the ceiling in an enclosed channel with different fire locations. *Appl. Therm. Eng.* **2017**, *111*, 30–38. [[CrossRef](#)]
10. Wang, X.; Wang, M.; Chen, J.; Yan, T.; Bao, Y.; Chen, J.; Qin, P.; Li, K.; Deng, T.; Yan, G. The maximum gas temperature rises beneath the ceiling in a longitudinally ventilated fire. *Tunn. Undergr. Space Technol.* **2021**, *108*, 103672. [[CrossRef](#)]
11. Peng, M.; Cheng, X.; Cong, W.; Yang, H.; Shahid, M.U.; Yuen, R.; Zhang, H. Experimental study on temperature profile in long-narrow compartment fire with multiple lateral openings. *Tunn. Undergr. Space Technol.* **2021**, *117*, 104018. [[CrossRef](#)]
12. Tsukahara, M.; Koshiba, Y.; Ohtani, H. Theoretical and experimental analysis of ceiling-jet flow in corridor fires. *Tunn. Undergr. Space Technol.* **2011**, *26*, 651–658. [[CrossRef](#)]
13. Wan, H.; Xiao, Y.; Wei, S.; Zhang, Y. Performance of ceiling jet induced by dual unequal strong plumes in a naturally ventilated tunnel. *Appl. Therm. Eng.* **2022**, *211*, 118447. [[CrossRef](#)]
14. Yi, L.; Lan, S.; Wang, X.; Bu, R.; Zhao, J.; Zhou, Y. Study on the air inlet velocity and temperature distribution in an inclined tunnel with single shaft under natural ventilation. *Buildings* **2023**, *13*, 842. [[CrossRef](#)]
15. Collela, F.; Rein, G.; Borchellini, R.; Carvel, R.; Torero, J.L.; Verda, V. Calculation and design of tunnel ventilation systems using a two-scale modeling approach. *Tunn. Undergr. Space Technol.* **2009**, *44*, 2357–2367. [[CrossRef](#)]
16. Oka, Y.; Oka, H.; Imazeki, O. Ceiling-jet thickness and vertical distribution along flat-ceilinged horizontal tunnel with natural ventilation. *Tunn. Undergr. Space Technol.* **2016**, *53*, 68–77. [[CrossRef](#)]
17. Kim, J.; Kim, K. Experimental and numerical analyses of train-induced unsteady tunnel flow in subway. *Tunn. Undergr. Space Technol.* **2007**, *22*, 166–172. [[CrossRef](#)]
18. Huang, Y.; Li, Y.; Li, J.; Dong, B.; Bi, Q.; Li, Y.; Li, J. Experimental investigation on temperature profile with downstream vehicle in a longitudinally ventilated tunnel. *Tunn. Undergr. Space Technol.* **2019**, *103*, 149–156. [[CrossRef](#)]
19. Tang, X.; Wang, M.; Tong, J.; Dong, C.; Zhang, C. Study on stress field and security of primary support in high rock temperature tunnel. *Tunn. Undergr. Space Technol.* **2019**, *54*, 32–38. [[CrossRef](#)]
20. Zhao, K.; Yuan, Y.; Jiang, F.; Cao, X. Numerical investigation on temperature–humidity field under mechanical ventilation in the construction period of hot-humid tunnel along the Sichuan-Tibet Railway. *Tunn. Undergr. Space Technol.* **2023**, *8*, 123–143. [[CrossRef](#)]
21. Gao, X.; Qu, Y.; Xiao, Y. A numerical method for the cooling and dehumidifying process of air flowing through a deeply buried underground tunnel with unsaturated condensation model. *Tunn. Undergr. Space Technol.* **2019**, *159*, 113891. [[CrossRef](#)]
22. Kang, F.; Li, Y.; Tang, C. Numerical study on the airflow temperature field in a high-temperature tunnel with insulation layer. *Tunn. Undergr. Space Technol.* **2020**, *179*, 115654. [[CrossRef](#)]
23. Wang, X.; Wang, M.; Chen, J.; Yan, T.; Bao, Y.; Chen, J.; Qin, P.; Li, K.; Deng, T.; Yan, G. A Study on the Heat Transfer of Surrounding Rock-Supporting Structures in High-Geothermal Tunnels. *Tunn. Undergr. Space Technol.* **2020**, *10*, 2307. [[CrossRef](#)]
24. Wang, Y. Case study on ventilation and cooling control technology of multi-heat source coupling in long-distance subsea tunnel construction. *Tunn. Undergr. Space Technol.* **2021**, *26*, 101061. [[CrossRef](#)]
25. Zhang, G.; Cao, Z.; Wang, W.; Mei, X.; Zhao, X.; Shen, S.; Na, T. Field test and numerical investigation on the thermal environment of a tunnel with air layer structure. *Tunn. Undergr. Space Technol.* **2021**, *203*, 108105. [[CrossRef](#)]

26. Lin, M.; Zhou, P.; Jiang, Y.; Zhou, F.; Lin, J.; Wang, Z. Numerical investigation on the comprehensive control system of cooling and heat insulation for high-geothermal tunnel: A case study on the highway tunnel with the highest temperature in China. *Tunn. Undergr. Space Technol.* **2022**, *173*, 107385. [[CrossRef](#)]
27. Wang, X. Feasibility Study on Cumulative Temperature Rise and Spray Cooling in Chongming Tunnel Operation. Master's Thesis, Tongji University, Shanghai, China, 2007.
28. Shan, M. Study on the Applicability of Natural Ventilation in Urban Underground Transportation Link Tunnels. Master's Thesis, Tongji University, Shanghai, China, 2015.
29. Guo, C.; Wang, M.; Yang, L.; Sun, Z.; Zhang, Y.; Xu, J. A review of energy consumption and saving in extra-long tunnel operation ventilation in China. *Renew. Sustain. Energy Rev.* **2016**, *53*, 1558–1569. [[CrossRef](#)]
30. Zhao, Z.; Xu, H.; Liu, G.; Liu, F.; Wang, G. A robust numerical method for modeling ventilation through long tunnels in high-temperature regions based on 1D pipe model. *Tunn. Undergr. Space Technol.* **2021**, *105*, 104050. [[CrossRef](#)]
31. Wang, X.; Wang, M.; Chen, J.; Yan, T.; Bao, Y.; Chen, J.; Qin, P.; Li, K.; Deng, T.; Yan, G. Analysis of calculation of fresh-air demand for road tunnel ventilation design in China. *Tunn. Undergr. Space Technol.* **2020**, *103*, 103469. [[CrossRef](#)]
32. Ciocanea, A.; Dragomirescu, A. Modular ventilation with twin air curtains for reducing dispersed pollution. *Tunn. Undergr. Space Technol.* **2013**, *37*, 180–198. [[CrossRef](#)]
33. Chu, B.; Kim, D.; Hong, D.; Park, J.; Chung, J.T.; Chung, J.H.; Kim, T.H. GA-based fuzzy controller design for tunnel ventilation systems. *Autom. Constr.* **2008**, *17*, 130–136. [[CrossRef](#)]
34. He, X.; Li, A.; Ning, Y. Optimization of outdoor design temperature for summer ventilation for undersea road tunnel using field measurement and statistics. *Build. Environ.* **2020**, *167*, 106457. [[CrossRef](#)]
35. Yang, C.; Luo, W.; Liu, Y.; Gao, R.; Zhang, S.; Li, A.; Du, W.; Zhang, B.; Zhang, J. A novel type of unpowered air curtain at a tunnel portal to reduce the intrusion of cold air. *Build. Environ.* **2022**, *218*, 109113. [[CrossRef](#)]

**Disclaimer/Publisher's Note:** The statements, opinions and data contained in all publications are solely those of the individual author(s) and contributor(s) and not of MDPI and/or the editor(s). MDPI and/or the editor(s) disclaim responsibility for any injury to people or property resulting from any ideas, methods, instructions or products referred to in the content.